Certifiably-Optimal Kinematically-Constrained Landmark-based SLAM

Michael Zeng, Toya Takahashi
Massachusetts Institute of Technology
77 Massachusetts Ave, Cambridge, MA 02139
michzeng@mit.edu, toyat@mit.edu

***Abstract*— We propose a certifiably optimal method for solving kinematically-constrained landmark-based SLAM. Given a set of stationary landmark locations in the robot frame at each timestep and assuming constant linear and angular velocity, our solver outputs the landmark locations in the world frame, along with the robot's pose and velocity at each timestep. In this paper, we first reformulate the problem from a non-linear least squares problem into a quadratically constrained quadratic program (QCQP). We then perform semidefinite relaxation on the QCQP and solve the resulting convex semidefinite program (SDP) to obtain a certificate of optimality. Additionally, we discuss the constraints required to tighten the relaxed problem. Finally, we demonstrate through simulated experiments that it tolerates realistic levels of measurement noise and can even produce accurate solutions in cases where the robot does not maintain a constant velocity.**

I. INTRODUCTION

Certifiable algorithms have proven effective in establishing guarantees on correctness across various areas of robotic perception, from object tracking [1] to 3D registration [2]. They are able to certify optimal solutions or declare failure on worst-case instances with a measurable optimality gap within polynomial time [3]. In this work, we propose an algorithm that extends this notion of optimality certification to landmark-based SLAM problems without odometry data, where the robot's motion is known to be roughly constant-twist (constant linear and angular velocity). This approach is well-suited for scenarios where the constant-twist assumption is reasonable, such as underwater exploration or autonomous vehicles operating on highways.

II. PROBLEM FORMULATION

A. MOTION AND MEASUREMENT MODEL

We represent the robot's state from its pose and velocity at a given timestep i. The translation component of the robot's pose at timestep i is denoted by $\mathbf{t}_i \in \mathbb{R}^3$, and the rotation by $\mathbf{R}_i \in \mathrm{SO}(3)$. Similarly, the robot's linear velocity at timestep j is denoted by $\mathbf{v}_j \in \mathbb{R}^3$ and angular velocity by $\mathbf{\Omega}_j \in \mathrm{SO}(3)$. The robot motion obeys the following discrete-time first-order dynamics:

$$\mathbf{t}_{i+1} = \mathbf{t}_i + \mathbf{R}_i \mathbf{v}_i, \qquad \mathbf{R}_{i+1} = \mathbf{R}_i \mathbf{\Omega}_i$$

Additionally, the measurement of landmark k at timestep i is denoted by $\bar{\mathbf{y}}_{k,i}$ where we assume the noise follows an isotropic zero-mean Gaussian distribution $\boldsymbol{\epsilon}_i^k \sim \mathcal{N}(0, \mathbf{\Sigma}_i^k)$.

B. LANDMARK-BASED SLAM FORMULATION

As a nonlinear least squares optimization problem, our problem takes the form

$$\begin{aligned} \min_{\substack{\mathbf{t}_i,\mathbf{v}_j,\mathbf{p}_k \in \mathbb{R}^3, \\ \mathbf{R}_i,\mathbf{\Omega}_j \in \mathrm{SO}(3), \\ i=1,\ldots,n, \\ j=1,\ldots,n-1, \\ k=1,\ldots,K}} & \sum_{k=1}^{K} \sum_{j \in \mathcal{S}_k} \|\bar{\mathbf{y}}_{k,j} - \mathbf{R}_j^T(\mathbf{p}_k - \mathbf{t}_j)\|_{\Sigma_\omega}^2 \\ & + \sum_{i=1}^{n-1} \|\mathbf{v}_{i+1} - \mathbf{v}_i\|_{\Sigma_\lambda}^2 + \sum_{i=1}^{n-1} \|\mathbf{\Omega}_{i+1} - \mathbf{\Omega}_i\|_{\Sigma_\kappa}^2 \\ \text{s.t.} \quad & \mathbf{t}_{i+1} = \mathbf{t}_i + \mathbf{R}_i \mathbf{v}_i, \ \ \mathbf{R}_{i+1} = \mathbf{R}_i \mathbf{\Omega}_i \end{aligned} \tag{1}$$

where N is the number of timesteps, K is the number of landmarks, and $\mathcal{S}_k$ is the subset of timesteps that observe landmark k. The first term minimizes the distance between the measured and estimated landmark locations in the robot frame. The second and third terms minimize change in twist, adding the constant-twist assumption in the objective.

Now, we reformulate this problem as a QCQP. Since the squared norm of $-\mathbf{R}_j^T(\mathbf{p}_k - \mathbf{t}_j)$ is quartic, we perform a simple trick utilized in [1] where we premultiply all terms inside the first norm by $\mathbf{R}_j$, which does not change the norm assuming isotropic covariance. Then, we express the $\mathrm{SO}(3)$ constraint as $\mathbf{R}_i^T \mathbf{R}_i = \mathbf{I}_3$ and $\mathbf{\Omega}_i^T \mathbf{\Omega}_i = \mathbf{I}_3$ where we drop the determinant constraint $\det(\mathbf{R}) = \mathbf{I}_3$. While this effectively performs optimization in $\mathrm{O}(3)$ rather than $\mathrm{SO}(3)$, the relaxation has been shown to be empirically tight for our case and for other problems [2]. Thus, the QCQP formulation of (1) is

$$\begin{aligned} \min_{\substack{\mathbf{t}_i,\mathbf{v}_j,\mathbf{p}_k \in \mathbb{R}^3, \\ \mathbf{R}_i,\mathbf{\Omega}_j \in \mathbb{R}^{3\times 3}, \\ i=1,\ldots,n, \\ j=1,\ldots,n-1, \\ k=1,\ldots,K}} & \omega \sum_{k=1}^{K} \sum_{j \in \mathcal{S}_k} \|\mathbf{R}_j \bar{\mathbf{y}}_{k,j} - \mathbf{p}_k + \mathbf{t}_j\|^2 \\ & + \lambda \sum_{i=1}^{n-1} \|\mathbf{v}_{i+1} - \mathbf{v}_i\|^2 + \kappa \sum_{i=1}^{n-1} \|\mathbf{\Omega}_{i+1} - \mathbf{\Omega}_i\|^2 \\ \text{s.t.} \quad & \mathbf{t}_{i+1} = \mathbf{t}_i + \mathbf{R}_i \mathbf{v}_i, \ \ \mathbf{R}_{i+1} = \mathbf{R}_i \mathbf{\Omega}_i \\ & \mathbf{R}_i^T \mathbf{R}_i = \mathbf{I}_3, \ \ \mathbf{\Omega}_j^T \mathbf{\Omega}_j = \mathbf{I}_3. \end{aligned} \tag{2}$$

Since the objective and the constraints are quadratic, we can rewrite (2) in the following form:

$$\begin{aligned} \min_{\tilde{\mathbf{x}} \in \mathbb{R}^{24n+3k-11}} \quad & \tilde{\mathbf{x}}^T \mathbf{Q} \tilde{\mathbf{x}} \\ \text{s.t.} \quad & \tilde{\mathbf{x}}^T \mathbf{A}_i \tilde{\mathbf{x}} + f_i = 0, \ i = 1, \ldots, m \end{aligned} \tag{3}$$

where $\tilde{\mathbf{x}} = [\mathbf{\Omega}_{1,\ldots,n-1}, \mathbf{R}_{1,\ldots,n}, \mathbf{p}_{1,\ldots,k}, \mathbf{v}_{1,\ldots,n-1}, \mathbf{t}_{1,\ldots,n}, y]$ subject to the quadratic constraint $y^2 - 1 = 0$. $\mathbf{Q}$ and $\mathbf{A}_i$ are

symmetric matrices defining the coefficients of the quadratic objective and constraints. y is a slack variable to homogenize $\mathbf{x}$ to include the linear terms in the equations.

Finally, we reparameterize the problem using $\tilde{\mathbf{X}} = \tilde{\mathbf{x}}\tilde{\mathbf{x}}^T$, a rank-1 positive semidefinite matrix. Then, using Shor's Semidefinite Relaxation, we drop the non-convex rank-1 constraint on $\tilde{\mathbf{X}}$ to obtain the following convex SDP:

$$\begin{aligned} \min_{\tilde{\mathbf{X}} \in \mathbb{S}^{24n+3k-11}} \quad & \text{trace}(\mathbf{Q}\tilde{\mathbf{X}}) \\ \text{s.t.} \quad & \mathbf{A}_i\tilde{\mathbf{X}} + f_i = 0, \;\; i = 1, \ldots, m \end{aligned} \tag{4}$$

After solving the SDP, we can recover the optimal solution by factorizing $\mathbf{X}^\star = \mathbf{x}^\star\mathbf{x}^{\star T}$ using its singular value decomposition. In addition, the rank of $\mathbf{X}^*$, if it is equal to 1, serves as a certificate of optimality; and when the solution is certified non-optimal, one can obtain a measure of sub-optimality using methods described in [3].

C. TIGHTENING THE RELAXATION

In addition to the basic formulation discussed above, there are several key constraints which were shown to tighten the relaxation.

a) Anchoring: To allow the SDP solver to converge to a single globally optimal solution, the initial robot pose was constrained: $\{\mathbf{t}_0 = \mathbf{0}, \mathbf{R}_0 = \mathbf{I}_3\}$.

b) Redundant Orthogonality Constraints: As discussed in [2], adding appropriate redundant constraints have shown to be effective for improving the quality of SDP relaxations. Thus, we add both column-based and row-based orthogonality constraints: $\{\mathbf{R}^T\mathbf{R} = \mathbf{I}_3, \mathbf{R}\mathbf{R}^T = \mathbf{I}_3\}$.

c) Separation of Linear Terms: Premultiplying the translation kinematics constraints by $\mathbf{R}_i^T$ yields $\mathbf{R}_i^T\mathbf{t}_{i+1} = \mathbf{R}_i^T\mathbf{t}_i + \mathbf{v}_i$. Then, the variables $\mathbf{v}_{1,\ldots,n-1}$ are linearly constrained, allowing us to separate out these terms in our problem formulation. Stacking the $\mathbf{v}_j$ terms in $\mathbf{v}$, we can rewrite 5 as follows:

$$\begin{aligned} \min_{\substack{\tilde{\mathbf{X}} \in \mathbb{S}^{21n+3k-8} \\ \mathbf{v} \in \mathbb{R}^{3n-3}}} \quad & \text{trace}(\mathbf{Q}\tilde{\mathbf{X}}) + \mathbf{v}^T\mathbf{P}\mathbf{v} \\ \text{s.t.} \quad & \mathbf{A}_i\tilde{\mathbf{X}} + \mathbf{d}_i^T\mathbf{v} + f_i = 0, \;\; i = 1, \ldots, m \end{aligned} \tag{5}$$

where $\mathbf{P}$ is a symmetric matrix defining the constant linear velocity objective and $\mathbf{d}_i$ captures the linear portions of the constraints. We noticed that this formulation empirically leads to a tighter relaxation which we suspect is due to the smaller problem size.

III. EXPERIMENTS

We evaluate our approach on five benchmark experiments illustrated in Fig. 1, that contain varying problem sizes and trajectories. The first four benchmark experiments follow the constant twist assumption exactly, while the fifth does not. In each benchmark, we vary the measurement noise standard deviation (STD) and run 10 trials, evaluating the resulting solution's rank, relaxation gap, errors relative to the ground-truth solution, and runtimes. In all trials, the robot's ground-truth linear velocity is precisely or very close to 1 unit/timestep.

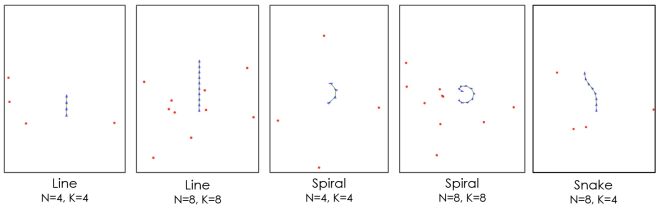

Fig. 1. Benchmark Test Cases

IV. RESULTS

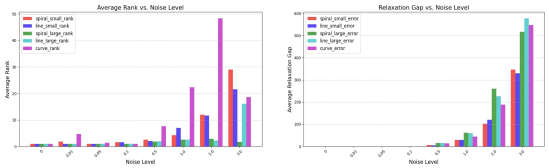

Fig. 2. Average Rank and Relaxation Gap

In Fig 2, we find that our algorithm returns solutions of rank 1 until very large measurement noise (0.5 or 1 unit STD). While the "Snake" benchmark, where constant twist assumptions do not hold, shows more sensitivity to noise than the others, our solver is able to return optimal solutions with high probability under reasonable noise. In most cases where the rank is not precisely 1 but close, we also find that the solution typically yields one dominant singular value, with potential numerical issues causing the discrepancy.

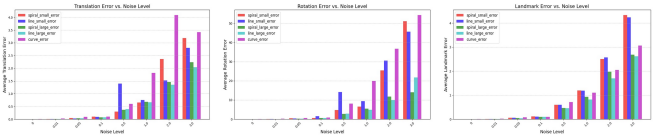

Fig. 3. Translation, Rotation (in deg.), and Landmark Position Errors

From Fig 3, we see similar trends, with the solutions' errors only becoming significant at high noise values of 0.5 units STD or above. Moreover, we find that even when the solutions are not certifiably optimal, they typically qualitatively resemble the ground-truth solutions, with catastrophic failures only occurring at extreme noise levels.

V. CONCLUSION & FUTURE WORK

We find that our method shows impressive resilience to measurement noise so long as the constant twist assumption is fairly accurate. The key limitation to our method is slow runtime due to the polynomial expansion of the SDP from the QCQP. Future work may work on integration of faster solvers that take advantage of the quadratic structure of the QCQP or integrating robust loss functions like truncated least squares to add robustness to outliers [4] [3].

VI. SOURCE CODE

Our code is open-source and is available here.

REFERENCES

[1] Shaikewitz, Lorenzo and Ubellacker, Samuel and Carlone, Luca. (2024). A Certifiable Algorithm for Simultaneous Shape Estimation and Object Tracking. 10.48550/arXiv.2406.16837.

[2] J. Briales and J. Gonzalez-Jimenez, "Convex Global 3D Registration with Lagrangian Duality," 2017 IEEE Conference on Computer Vision and Pattern Recognition (CVPR), Honolulu, HI, USA, 2017, pp. 5612-5621, doi: 10.1109/CVPR.2017.595.

[3] Yang, Heng and Luca Carlone. "Certifiably Optimal Outlier-Robust Geometric Perception: Semidefinite Relaxations and Scalable Global Optimization." IEEE Transactions on Pattern Analysis and Machine Intelligence PP (2021).

[4] Yang, Heng and Liang, Ling and Carlone, Luca and Toh, Kim-Chuan. (2021). An Inexact Projected Gradient Method with Rounding and Lifting by Nonlinear Programming for Solving Rank-One Semidefinite Relaxation of Polynomial Optimization. 10.48550/arXiv.2105.14033.